Low-energy nano-emulsification approach as a simple strategy to prepare positively charged ethylcellulose nanoparticles

S.Leitner[1], C. Solans[1], M.J. García-Celma[2,1], G. Calderó[1]

[1] Institut de Química Avançada de Catalunya (IQAC-CSIC). Jordi Girona 18-26, 08034 Barcelona, Spain. Centro de Investigación Biomédica en Red en Bioingeniería, Biomateriales y Nanomedicina (CIBER-BBN), Barcelona, Spain

[2] Departament de Farmàcia i Tecnologia Farmacèutica i Fisicoquímica. IN2UB.Univ. de Barcelona. Unitat Associada d'I+D al CSIC- Av Joan XXIII, s/n, 08028 Barcelona, Spain

ABSTRACT

Positively charged ethylcelulose nanoparticles have been obtained from alkylamidoammonium/Span 80 based nano-emulsion templates. Oil-in-water polymeric nano-emulsions form in a broad range of oil-to-surfactant ratios and water contents above 75 wt% by a low-energy method at 25ºC. Nano-emulsions with a water content of 90 wt% showed droplet sizes typically below 300 nm and high positive zeta potential values (~55 mV). If oleylamine is added to the system, smaller droplet sizes and higher zeta potential values (~66 mV) are obtained, but the stability of the nano-emulsions decreases. Although these nano-emulsions are destabilized by creaming, the period of stability is large enough to allow nanoparticle preparation by solvent evaporation. Polymeric nanoparticles obtained show a globular core-shell-like morphology, with mean diameters of around 250 nm. The surface charge of the nanoparticles is similar to that of the nano-emulsion template and remains positive after 24 hours dialysis, suggesting slow desorption kinetics of the alkylamidoammonium from the nanoparticle surface. These results indicate that the proposed nano-emulsion approach is a good strategy for the preparation of positively charged nanoparticles from nonionic ethylcellulose polymers.

KEYWORDS

Cationic nano-emulsion; ethylcellulose nanoparticles; cationic nanoparticles; low-energy emulsifiaction

1. INTRODUCTION

Positively charged nanoparticles have attracted the interest of biomedical researchers for their ability to bind anionic drugs (especially nucleic acid derivatives for gene therapy) to form stable complexes and the advantageous properties generally attributed to positively charged nanomaterials such as mucoadhesivity and antimicrobial activity **[1-6]**. For this purpose, polycations like chitosan **[7]**, poly(ethyleneimine) or poly(amidoamine) **[3, 8]** have been extensively studied. Nanoparticles prepared with non-charged or anionic materials usually display close to zero or negative zeta potential values. This has been described for example for nanoparticles of ethylcellulose **[13]**, poly(lactic-co-glycolic) acid **[12]** or solid lipid nanoparticles **[14]**. To confer a positive surface charge to these kinds of materials, strategies such as covalent binding of cationic molecules have been proposed. For example, Fornaguera et al. achieved changing the surface charge of poly(lactic-co-glycolic) acid (PLGA) nanoparticles from negative (about - 20 mV) to positive values (as high as about + 70 mV) by covalently binding cationic carbosilane dendrons to the nanoparticle surface **[9]**. An interesting alternative to covalent attachment is the adsorption of cationic molecules onto the nanoparticle surface. Nanoparticles can be endowed with modified surface properties such as hydrophilicity, cationic charge and so on, by incubating them with selected molecules which would adsorb onto their surface. This has been shown with polar molecules, such as PEG derivatives **[10]**, polysorbate 80 **[11]** or chitosan **[12]**, which are usually added in a late step, after nanoparticle preparation as an alternative to covalent linking.

A well-known method for nanoparticle preparation is nano-emulsion templating. The preparation of nano-emulsions by low-energy methods is convenient because it allows achieving smaller and more homogeneous droplet sizes than high energy emulsification methods. Although the preparation of O/W nano-emulsions with nonionic surfactants by low-energy emulsification methods has widely been studied **[15-18]**, only a limited number of papers have been devoted to nano-emulsion

preparation by low-energy methods using ionic surfactants or mixtures of cationic and nonionic surfactants **[19-21]**. The incorporation of a cationic surfactant or the use of mixed ionic-nonionic surfactant systems may be beneficial for certain biomedical applications and may as well contribute to the so called electrosteric stabilisation, i.e. both, electrostatic and steric repulsion for stabilizing the dispersed droplets **[22]**. In previous papers by our group, we have demonstrated the high versatility of the low-energy nano-emulsion approach for the preparation of polymeric nanoparticles (ethylcellulose **[17]** and PLGA **[23]**) with a broad range of characteristics such as size (e.g. hydrodynamic radii from 20 nm to 200 nm), loading (dexamethasone **[32]**, loperamide **[25]**, galantamine **[26]**) or functionality (binding of transferrin receptor targeting 8D3 antibody **[25]** or of cationic carbosilane dendrons for gene therapy **[9]**). These ethylcellulose and PLGA nanoparticles have been prepared using nonionic ethoxylated surfactants, and display a negative surface charge (typically between about -20 mV and -70 mV) unless the nanoparticle surface is functionalized with covalently bound cationic dendrons **[27]**.

In this context, in the present research work it is hypothesized that positive surface charge may be conferred to ethylcellulose nanoparticles prepared using the low-energy emulsification approach by introducing a cationic amphiphilic compound, namely an alkylamidoammonium derivative, before nanoparticle preparation, with no chemical reaction and no additional post-adsorption steps. This method presents the advantage of avoiding the use of potentially toxic reactants and time consuming purification steps although it might be less effective due to easy desorption. The cationic surfactant is expected both, to adsorb at the water/polymer interface due to its dual hydrophilic-hydrophobic nature and to interact with the nonionic polymer thus generating a positive surface charge. It is worth mentioning that monomeric alkylamidoammonium derivatives are a class of cationic surfactants which in spite of their frequent use in the home and personal-care industry have not been explored yet, to our best knowledge, for biomedical applications. In contrast to their amidoamine counterparts, they have the advantage of being permanently positively charged, regardless of the pH of the dispersing medium, due to the quaternized ammonium end group. In this paper we propose the preparation of positively charged nanoparticles from ethylcellulose nano-emulsion templates formed in a mixed cationic/nonionic surfactant system. The purpose of this paper is to explore the

feasibility of endowing positive surface charge to ethylcellulose nanoparticles prepared by a low-energy emulsification-solvent evaporation method, by using a cationic alkylamidoammonium surfactant to modulate the surface charge of the nanoparticles, and assess its permanence when exposed to a diluting medium.

2. EXPERIMENTAL

2.1. Materials

Ethylcellulose, a commercial semi synthetic cellulose ether derivative, was from Colorcon, a distributor of the Dow Chemical Company (ETHOCEL™ Premium Std 10 ethylcellulose polymer, abbreviated as EC10. ETHOCEL is a trademark of the Dow Chemical Company). This polymer is insoluble in water. It consists of repeating anhydroglucose units in which hydroxyl groups have been partially substituted by ethoxyl groups. Ethoxyl content was 48.7% and the weight-average molecular weight (Mw) was 66385 ± 322 Dalton with a polydispersity of 4.3 as determined by Gel Permeation Chromatography (see Supplementary Information for analysis conditions). Ethyl acetate (> 99.8%), supplied by Merck, was used as organic solvent. This solvent has a boiling point of 77 ºC, it is partially soluble in water and can dissolve water up to 3 wt% at 25ºC **[17]**. The cationic alkylamidoammonium amphiphile, ricinoleamidopropyltrimonium methosulfate (**Figure 1**), in the following abbreviated as CatA, was from Evonik. This technical grade cationic surfactant has an active matter content of 40 wt% in water. It is fluid at room temperature and appears clear yellow with tendency to cloudiness at 20°C. It has a density of 1.03 g/cm^3 at 20 °C and is easily soluble in water at room temperature. It is generally used in the formulation of commercial home and personal care products. It has a critical micellar concentration of 3.3 x 10^{-2} mM **[28]**. Sorbitan monooleate (Span® 80) and oleylamine (≥ 70%, GC) were purchased from Fluka. Sorbitan monooleate is a nonionic, yellow, at room temperature liquid surfactant, with a hydrophilic-lipophilic balance (HLB) number of 4.3. Oleylamine is a slightly yellow and clear liquid with a melting point of 18 – 26ºC, a density of 0.813 g/mL and a boiling point of 348 – 350ºC. Water was

deionized and MilliQ® filtered. When stated in the text, phosphate buffer 0.02M (abbreviated PB) was used as diluting medium.

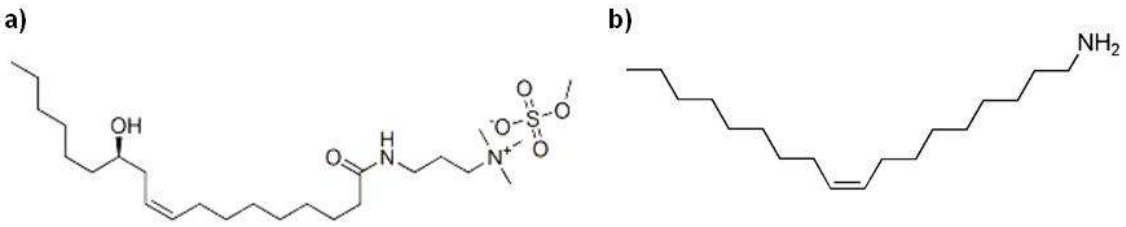

Figure 1: Chemical structure of a) ricinoleamidopropyltrimonium methosulfate (CatA) and b) oleylamine (OA).

2.2. Methods

2.2.1. Phase Inversion determination

The phase inversion region was determined by conductivity measurements. Samples (4 g) were prepared by addition of water to oil/surfactant mixtures up to 90 wt%. Electrical conductivity of samples was measured at each composition by means of a Crison-GLP 31 conductimeter with a Pt/platinized electrode under continuous magnetic stirring at 25ºC.

2.2.2. Formation of oil-in-water (O/W) nano-emulsions

About 4 g of the nano-emulsions were prepared at a constant temperature of 25°C by adding water dropwise to the mixture of oil and mixed surfactants, which was previously homogenized. The addition was performed under permanent vortex stirring (Vortex Genie 2^{TM}, Scientific Industries Inc.) at about 2700 rpm.

2.2.3. Nano-emulsion region determination

The region of formation of O/W nano-emulsion in the Water / [cationic:nonionic surfactant mixture] / oil system was at first assessed visually at 25°C. Samples with various O/S ratios and water contents were prepared as described in **Section 2.2.2**. Compositions with a translucent to opaque appearance and a reddish or bluish shine when observed through a lamp light were identified as nano-emulsions.

2.2.4. Nanoparticle preparation

Nanoparticles were prepared by the solvent evaporation method using a rotary evaporator (Büchi) during 45 minutes under reduced pressure of 43 mbar and at 25°C. After evaporation, weight loss was replaced with water. The volume shrinking factor from nano-emulsion droplet to nanoparticle has been determined from the ratio of the volumes of the droplets and the nanoparticles calculated from the hydrodynamic size as obtained by dynamic light scattering measurements, assuming that the number of dispersed entities keeps constant. The theoretical diameter of nanoparticles was determined from the hydrodynamic diameter of the nano-emulsion droplets by considering the volume of dispersed spheres, assuming that the number of dispersed entities keeps constant during the evaporation process, that no water is present in the dispersed phase and that once evaporation is completed, nanoparticles consist exclusively of polymer. For the calculation, densities of ethyl acetate and ethylcellulose were taken to be 0.9 g/mL and 1.15 g/mL respectively.

2.2.5. Particle size characterization

Dynamic light scattering: Droplet (nano-emulsions) and particle (nanoparticle dispersion) size were determined by Dynamic Light Scattering (DLS) with a Photon Correlation Spectrometer (PCS) from Malvern Instruments, equipped with an Argon laser (λ = 488 nm). Results were given as ZAverage (ZAve) which corresponds to the hydrodynamic droplet or particle diameter. Nano-emulsions and nanoparticle dispersions were diluted (1/100) with water saturated with ethyl acetate (refractive index of 1.349) in order to prevent diffusion of ethyl acetate from the droplets to the continuous phase and water (refractive index of 1.333) respectively. Measurements were carried out as triplicates at a scattering angle of 90°, at 25°C.

Transmission Electron Microscopy (TEM): Nanoparticle size was also determined by using the transmission electron microscope JEOL JEM 1010 (Jeol Korea Ltd.), operating at 80 kV. The samples were prepared just after solvent evaporation. A drop of the nanoparticle dispersion was placed on a carbon coated cupper grid and then negatively stained with 2 wt% uranyl acetate (UA) solution. About 1000 particles were sized manually from about 50 TEM micrographs taken at different magnifications. For this purpose, the software package Image J was used. Data were evaluated with the Origin software package for particle size distribution calculation.

2.2.6. Nano-emulsion and nanoparticle dispersion stability

Macroscopic observation: Nano-emulsions and nanoparticle dispersions were kept in a glass vial in a thermostated bath at 25°C. They were visually checked as a function of time.

Light Backscattering: Stability of the nano-emulsions was also assessed by light backscattering measurements with a TurbiscanLab® Expert instrument, at 25ºC. 15 g of freshly prepared sample were transferred into the glass cell which was tightly stoppered in order to prevent solvent evaporation. A pulsed near infrared LED (λ = 880 nm) served as light source. The instrument consists of two synchronous optical sensors, one receiving light transmitted through the sample and the other one receiving light backscattered by the sample at an angle of 135º. Data were acquired each hour during 24 hours at 25°C. The destabilization rate was determined by plotting the destabilization index (*DI*) as a function of time. *DI* is a statistical factor provided by the Turbisoft 2.1.0.52 software, computed from the sum, in absolute value, of the variation of each selected scan of a sample at a given time and sample height to the previous one, according to the following expression:

$$Destabilization\ index(\ DI) = \sum_i \frac{\sum_h \left| scan_i(\ h) - scan_{i-1}(\ h) \right|}{H} \quad \text{(Eq. 2)}$$

where *i* is a measurement at a given time, *h* is the sample height in the measuring cell, $scan_i(h)$ is the scattering (transmission or backscattering) value at the considered sample height in the measuring cell at a given time; $scan_{i-1}(h)$ is the scattering value at the same sample height obtained in the previously considered measuring time; and *H* is the total sample height in the measuring cell. Analysis was performed considering scattering variations over the whole sample height range. The higher the value of *DI*, the more unstable the dispersed system.

2.2.7. Nano-emulsion and nanoparticle surface charge

The zeta potential, a measure of the net surface charge, was determined from the electrophoretic mobility measured on a ZetaSizer Nano Z laser diffractometer (Malvern Instruments), by applying the Smoluchowsky equation **[29]**. For the measurements, nano-emulsions were diluted with water to a concentration of 20 mg

nano-emulsion /g solution. Each sample was measured in triplicate at room temperature.

2.2.8. Removal of surfactant excess from nanoparticle dispersion by dialysis

About 4 g of nanoparticle dispersion were filled in a SpectraPor dialysis bag (MWCO of 12000 – 14000) and immersed in 800 mL of MilliQ filtered water at 25ºC. The conductivity in the dialysate solution was monitored by means of a Crison-GLP 31 conductimeter with a Pt/platinised electrode. The dialysate was replaced twice, after 30 minutes and after 2 hours, and was then allowed to equilibrate until conductivity in the dialysate solution reached a plateau. Conductivity data were automatically collected on a computer every 5 minutes in the first dialysate, every 15 minutes in the second one and every 60 minutes in the third one.

3. RESULTS AND DISCUSSION

3.1. Nano-emulsion formation and characterization

The formation of oil-in-water (O/W) nano-emulsions has been studied in the Water / [CatA:Span® 80] / [6% EC10 in ethyl acetate] system at 25ºC as described in **Section 2.2.2**. For this purpose, first the oil component and the surfactants are thoroughly mixed, and then, the water is dropwise added up to the required amount under continuous stirring. The ratio CatA:Span® 80 was 1:1 and the concentration of ethylcellulose in ethyl acetate was 6 wt%. **Figure 2** shows that nano-emulsions are obtained in a wide range of oil/surfactant (O/S) ratios, between 25/75 and 85/15, and at water contents above 75 wt% (purple area). The higher the water content the more transparent they appeared. It is worth noting that they could be formed at O/S ratios higher than those obtained in other systems by low-energy emulsification methods in the absence of polymer and using a less polar oil. In those systems nano-emulsions could not be formed at O/S ratios higher than 40/60 **[18, 30]**. In the system shown here, the O/S range of nano-emulsion formation is even broader than that found in systems with the same oil components **[17, 24]**. It is worth mentioning that nano-emulsions were only obtained if the surfactant was first mixed with the oil.

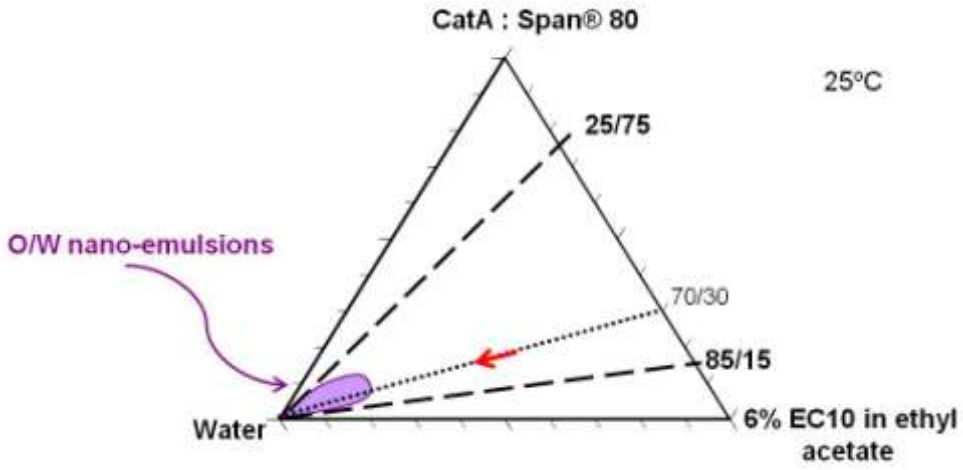

Figure 2. Oil-in-water (O/W) nano-emulsion region (purple area close to the water vertex) in the Water / [CatA:Span® 80 = 1:1] / [6 wt% EC10 in ethyl acetate] system, at 25ºC. The dashed lines at O/S ratios of 25/75 and 85/15 are a guide to the eye indicating the O/S ratio boundary of nano-emulsion formation. The dotted line with the red arrow for the O/S ratio 70/30 indicates the dilution path which was followed for conductivity measurements. Samples were prepared by addition of the aqueous component to the mixture of the oil and the surfactants.

The occurrence of phase inversion from O/W type to W/O type systems along the emulsification path was verified by conductivity measurements at 25ºC, as described in **Section 2.2.1**. **Figure 3** shows the conductivity (**Figure 3a**) as a function of total water content along the dilution path with O/S ratio of 70/30 (dotted line in **Figure 2**) and the destabilization kinetics (**Figure 3b**) of nano-emulsion samples at 25ºC as determined from the destabilization index (*DI*) as a function of time. *DI* is a statistical factor which is obtained from the transmission and light backscattering spectra of the samples as explained in section 2.2.6.

. .

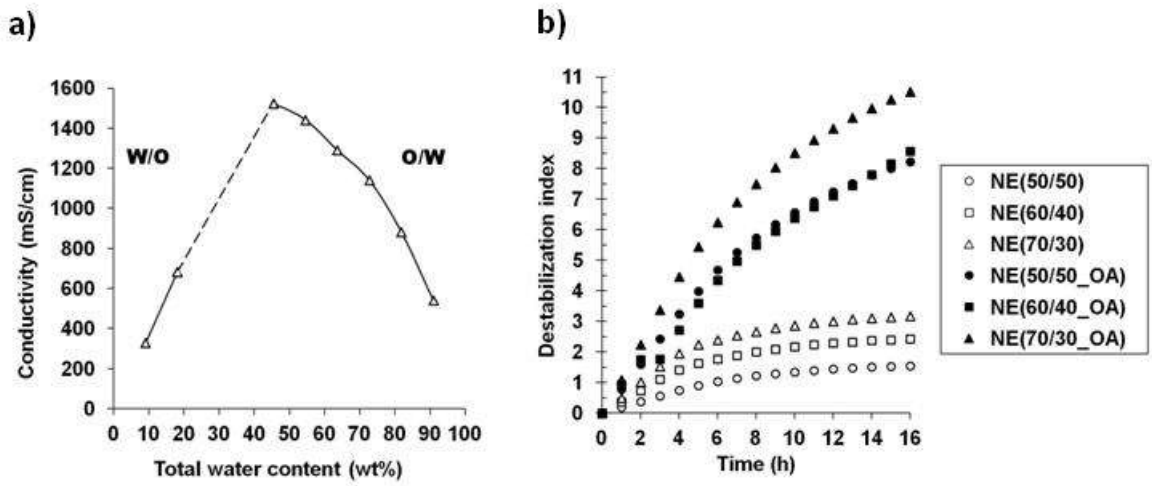

Figure 3. a) Conductivity as a function of total water content in the Water / [CatA:Span® 80 = 1:1] / [6 wt% EC10 in ethyl acetate] system along the dilution path at the O/S ratio 70/30, at 25ºC. The dashed line indicates the region of instable samples which could not be measured. Water-in-oil (W/O) and oil-in-water (O/W) regions are indicated. b) Destabilization kinetics of nano-emulsion samples at 25ºC as determined from the destabilization index (*DI*) as a function of time.

The amount of water present in the surfactant CatA (40 wt% of active matter) was considered in the total water content in the plot. For that reason, the lowest water concentration that could be studied was about 9 wt% of water. At low water contents, conductivity values increase upon increasing water concentration. Conductivity between about 20 and 40 wt% of water could not be measured accurately due to fast phase separation of the samples. Conductivity values reach a maximum at about 45 wt% of water and then gradually decrease. The increase in conductivity at low water content is indicative of water-in-oil (W/O) structures which experience a transition at higher water concentration. The decrease in conductivity is indicative of the dilution effect of the conducting species present in the system **[31, 32]**. Bell-shaped curves as obtained here had previously been described in literature **[17, 31, 32]**. Inversion from W/O to O/W takes place during emulsification. However, there is a remarkable difference between conductivity values of nano-emulsions of the present study and those of similar systems formulated with a nonionic surfactant **[17]**. While conductivity in this system was close to zero at water contents of 0 – 20 wt% and reached a maximum value of about 320 μS/cm at 42 wt% water contents,

conductivity values in the present system are quite high due to the presence of the cationic surfactant.

Nano-emulsions with O/S ratios of 50/50, 60/40 and 70/30 and a water content of 90 wt% were selected for further studies (NE(50/50), NE(60/40) and NE(70/30) respectively). To enhance the cationic properties of the system, oleylamine (OA) was incorporated in these nano-emulsions (NE(50/50_OA), NE(60/40_OA) and NE(70/30_OA). This fatty amine has a pK_a of about 10.7 **[33]** and is consequently positively charged at lower pH values. It was mixed with the oil component in the ratio [EC10 in ethyl acetate]:oleylamine of 3:1. Characteristics of nano-emulsions prepared with and without this component are summarized in **Table I**.

Table I. pH values, ZAverage droplet size and polydispersity indices (PI) of nano-emulsions of the Water / [CatA:Span® 80 = 1:1] / [6 wt% EC10 in ethyl acetate] system with 90 wt% of water content at 25°C. Electrophoretic mobility (**μ**) and zeta potential (**ζ**) values of nano-emulsions of the system in water (pH 5.6) and PB (pH 7.4) as diluting media, at a concentration of 20 mg/g, at room temperature.

[6%EC10 in ethyl acetate] : OA	O/S ratio	pH[(1)]	ZAve (nm)[(2)]	PI[(2)]	μ (μmcm/Vs)		ζ (mV)	
					Water[(3)]	PB[(3)]	Water[(3)]	PB[(3)]
1:0	50/50	5.1	297.6	0.12	4.8	2.3	61.1	28.2
	60/40	5.2	305.1	0.15	4.3	2.0	55.3	25.2
	70/30	5.5	261.7	0.10	4.3	1.6	55.1	20.5
3:1	50/50	8.6	250.7	0.14	5.1	2.7	65.1	34.8
	60/40	9.2	238.9	0.10	5.3	2.8	67.9	35.8
	70/30	9.3	230.8	0.13	5.4	2.8	68.0	36.3

[(1)]pH values of as-prepared nano-emulsions. [(2)]Droplet size and polydispersity index (PI) obtained with DLS upon dilution (1/100) with water saturated with ethyl acetate

(3) Diluting medium to attain a final concentration of 20mgEC10/g (pH values of water and PB are 5.6 and 7.4 respectively).

In the absence of oleylamine, the pH values of the nano-emulsions where moderately acidic while pH values of the systems with OA increase up to around 9. It was found that the pH value increases slightly with the O/S ratio. In samples containing the fatty amine, this increase is consistent with the higher amount of oleylamine when the O/S ratio increases. The nano-emulsion with and without fatty amine were characterized by DLS (**Section 2.2.5**). Nano-emulsions without OA show mean droplet sizes (ZAve) up to around 300 nm and polydispersities below 0.15 at room temperature. In the presence of oleylamine, however, droplet sizes decreased to around 240 nm, showing similar polydispersities than those of the system without OA. Furthermore, a decrease of droplet sizes with the increase of O/S ratio is noticeable which may be due to the presence of fatty amine placing itself at the interfacial surfactant film and acting as a cosurfactant, as this molecule consists of a polar head group and a hydrocarbon chain and may therefore display amphiphilic character. In addition, it is probable that the effect of solvent diffusion from the droplets towards the continuous phase leading to a decrease in droplet size dominates over the increase in droplet size produced by an increase in dispersed fraction. By contrast, no clear tendency in droplet size as a function of the O/S ratio is observed in nano-emulsions without OA. Nevertheless, the smallest droplet size was achieved at the highest O/S ratio (70/30) which may be attributed to solvent diffusion.

The surface charge of the nano-emulsion droplets was determined by zeta potential measurements. To allow proper measurements, the nano-emulsions were diluted. In a first step, the effect of the degree of dilution and the nature of the diluting medium water and a phosphate buffer solution, PB 0.02M) were determined. The buffer was used in order to study influences on the nano-emulsion system at physiological pH (pH 7.4 of human blood). **Figure 4** shows the results. When diluting in water, zeta potential increased with increasing nano-emulsion concentration from slightly negative values (about -1 mV) until a plateau was nearly reached in the positive range (about +54 mV). Using PB as diluting media, zeta potential values showed a similar tendency, starting with negative values at low concentration and raising to higher positive values with increasing concentration. However, values in water (pH = 5.6) are generally about 20 mV higher than in PB (pH = 7.4) in the studied dilution range. The reason may be that the phosphate anionic species in the buffer solution

shield the cationic charges provided by the surfactant CatA, producing a decrease of the zeta potential values.

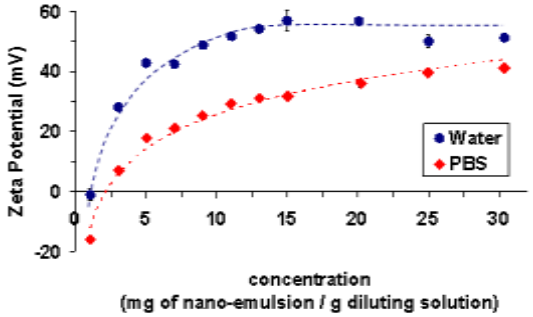

Figure 4: Zeta potential of the nano-emulsions of the Water / [CatA:Span® 80 = 1:1] / [6 wt% EC10 in ethyl acetate] system as a function of the concentration of nano-emulsion in the diluting medium (water (pH = 5.6) or PB (pH=7.4)), at 25°C. The nano-emulsion composition was O/S ratio 60/40 and 90 wt% water. The symbols are the experimental data and the lines a guide to the eye.

Based on these results, further measurements were performed by diluting to a concentration of 20 mg/g, which is within (diluting medium: water) or close to (diluting medium: PB) the plateau range. As previously observed, one main factor affecting the zeta potential seems to be the diluting medium (**Table I**). The presence of anionic shielding species strongly decreases the zeta potential. While in water the zeta potential is around 60 mV, in PB this value drops down to about the half. Furthermore, with all diluted systems containing OA the zeta potential values are higher than without this component. This implies that these nano-emulsions contain more cationic charge caused by the presence of the OA carrying a positive charge at the studied pH values. A slight decrease in zeta potential with increasing oil content can be observed in the systems without OA with both diluting solvents due to the decrease in CatA content. However, in the presence of oleylamine surface charge of nano-emulsions keeps almost constant. It may be assumed that the decrease in CatA with increasing O/S ratio is compensated by the cationic charge provided by the fatty amine as this component is added to the oil phase.

Due to high zeta potential values of the studied nano-emulsions, a good stability is expected as a result of electrostatic repulsion among droplets. Yet the visual

assessment of the samples stored at room temperature reveals that a layer in the upper part of the sample is formed at about seven hours after nano-emulsion preparation, indicating creaming. For a closer analysis, tests by light backscattering were undertaken. **Figure 5** displays the results for the nano-emulsion with an O/S ratio of 70/30 with and without oleylamine. The backscattering intensity (expressed in percentage compared to internal standards) is plotted as a function of sample height (horizontal axis) at different times. In the sample without OA, a slight increase in backscattering intensity is observed at the bottom of the cell which is due to multiple light diffractions of the glass cell (**Figure 5a**). No physical meaning is assigned to this phenomenon. Backscattering intensity did not change throughout the sample height during 24 hours indicating, that clarification of the continuous phase, caused by a decrease in droplet size or in quantity of dispersed droplets, does not occur. However, at the meniscus, a peak appeared after three hours which is an indication of creaming.

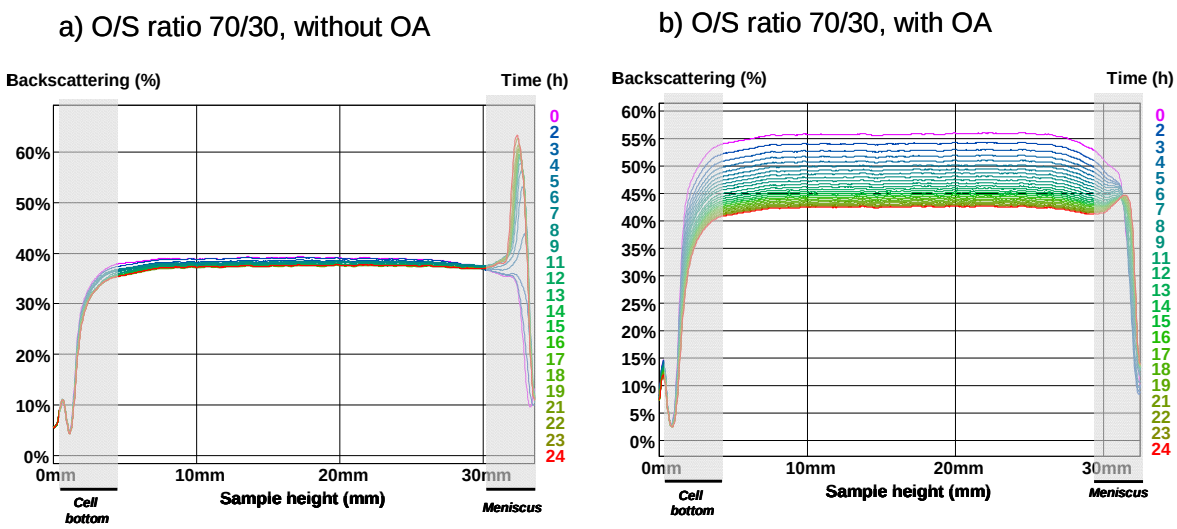

Figure 5: Backscattering data of the nano-emulsion of the Water / [CatA:Span® 80 =1:1] / [6 wt% EC10 in ethyl acetate] system with an O/S ratio of 70/30 and 90 wt% water **a)** in the absence and **b)** in the presence of oleylamine (OA), at 25ºC. The grey shaded regions in the graphics indicate the bottom and meniscus of the sample in the glass cell.

Table II Stability assessment of the three selected O/S ratios of nano-emulsions of the water / [CatA:Span® 80] / [6 wt.% EC10 in ethyl acetate] system without and with oleyl amine (OA) as determined by visual observation and light backscattering at 25ºC, and calculated from Stokes' law.

[6%EC10 in ethyl acetate] : OA	O/S ratio	Visual assessment of phase separation (h)	Backscattering appearance of a peak in meniscus (h)	Theoretical creaming rate (nm/s)	
				Assuming no solvent diffusion	Assuming solvent diffusion
1:0	50/50	≤ 7	-	- 4.5	8.0
	60/40	≤ 7	5	-4.7	8.5
	70/30	≤ 7	3	-3.5	6.2
3:1	50/50	< 7	1	-4.2	-5.2
	60/40	< 7	1	-3.8	-4.7
	70/30	< 7	1	-3.5	-4.4

With the sample containing OA (**Figure 5b**) the backscattering intensity increase at the meniscus of the samples is significantly reduced compared to the nano-emulsions in the absence of OA which is in good agreement with the lower creaming rate predicted by Stokes' law (**Table II**). However, a striking decrease in the backscattering intensity is observed with time. This phenomenon has been related to a clarification of the continuous phase, which can be caused by a decrease in the size or in the number of the dispersed droplets. On the one hand, a decrease in size can be caused by the diffusion of the partially water-soluble ethyl acetate from the dispersed droplets to the aqueous continuous phase. On the other hand, a decrease of the number of dispersed entities can occur as a consequence of coalescence, flocculation or Ostwald ripening. Since nano-emulsions showed high surface charge values, flocculation and coalescence of the droplets should not be favorable here. Ostwald ripening however, which implies a growth of the larger droplets at an expense of the smallest ones is prone to happen in polydisperse nano-emulsion systems and would lead to a reduction of the number of drops. The clarification observed and identified as Ostwald ripening, which started right in the first hour after sample preparation, can be regarded as consistent with the visual observation of samples where creaming was observed 7 hours after sample preparation. As mentioned before, destabilization is likely to take place before this time. Similar results were obtained for the nano-emulsions with O/S ratios 50/50 and 60/40 in absence and presence of the fatty amine. Overall destabilization kinetics (**Figure 3b**) clearly confirms the lower stability of the nano-emulsions in the presence of OA in spite of the contribution of this component to higher positive surface charge of the droplets. These stability results are in agreement with the visual assessment.

3.2. Nanoparticle formation and characterization

The nano-emulsion with the O/S ratio of 70/30 was selected for nanoparticle formation as it showed the smallest droplet size, with high zeta potential values and a stability assessed visually similar to the other compositions (O/S ratio 50/50 and 60/40) and sufficient for nanoparticle preparation. The polymeric nanoparticles were obtained from the nano-emulsion by solvent evaporation under reduced pressure as

451 described in **Section 2.2.4**. The characteristic nanoparticle diameter, determined by
452 DLS, was 202 nm. This value is smaller than that of the template nano-emulsion
453 attributed to the evaporation of ethyl acetate from the droplets during nanoparticle
454 preparation. The shrinking factor of the droplets upon nanoparticle formation as
455 calculated from light scattering data is about 2.2. However, the expected reduction in
456 size would be larger (to a nanoparticle diameter of about 100 nm), as calculated from
457 the nano-emulsion hydrodynamic radius, considering that the number of dispersed
458 entities keeps constant during evaporation, that no water is present in the dispersed
459 phase and that once evaporation is completed, nanoparticles consist only of polymer.
460 This may be an indication that during the evaporation process, destabilization
461 phenomena such as Ostwald ripening or flocculation and/or coalescence may take
462 place. The observation of the nanoparticle dispersion by transmission electron
463 microscopy (TEM) revealed that the nanoparticles display a globular core-shell like
464 morphology and are partially aggregated (**Figure 6a**). The core-shell appearance is
465 due to the penetration of the negative stain in the outer layer of the nanoparticles,
466 which may be due to the higher hydrophilic character of the adsorbed cationic
467 surfactant. Their diameter by TEM of about 230 nm roughly matches with the mean
468 particle diameter obtained by DLS.
469

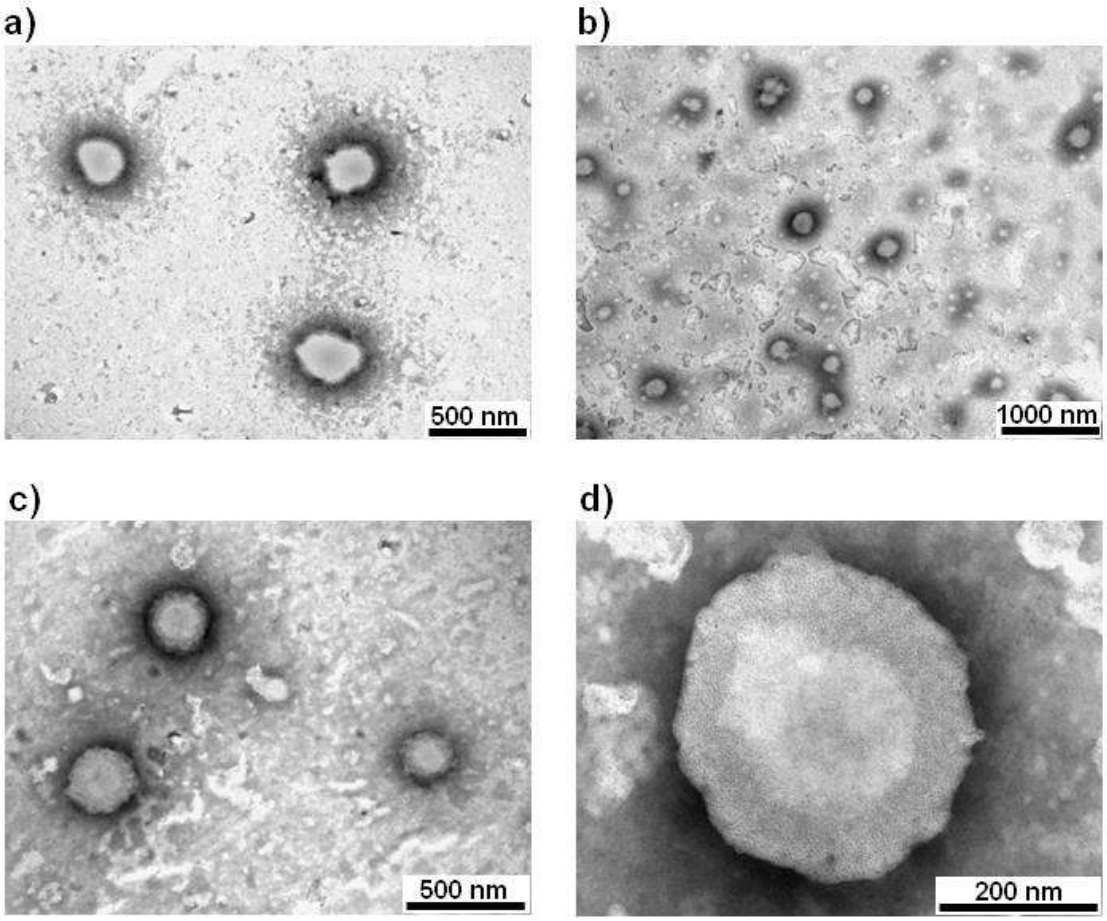

Figure 6. TEM micrographs of a negatively stained nanoparticle dispersion obtained from the nano-emulsion of the Water / [CatA:Span® 80 =1:1] / [6 wt% EC10 in ethyl acetate] system with an O/S ratio of 70/30 and 90 wt% water **a)** and **b)** before dialysis and **c)** and **d)** after dialysis.

The nanoparticle dispersion obtained was dialyzed in order to remove excess of surfactant and assess the residual positive charge remaining on the surface of the nanoparticles. The dialysis process was performed as described in **Section 2.2.8** and was followed by conductivity measurements (**Figure S1**). The conductivity of MilliQ water was 2.64 μS/cm. The conductivity detected in the dialysate was considered to be caused by the diffusion of the cationic surfactant, as it is the main conducting species in the nanoparticle dispersion. The contribution of other components or impurities to the conductivity was neglected. The cationic surfactant molecules most prone to be removed by diffusion are those available in the monomeric form in the aqueous continuous phase of the nanoparticle dispersion and/or those only weakly adsorbed on the nanoparticle surface. Therefore, the

cationic surfactant remaining in the nanoparticle dispersion after dialysis is believed to be that stronger adsorbed on the surface of the nanoparticles. This may happen by entanglement of the hydrophobic chain of cationic surfactant into the polymeric matrix of the nanoparticle, allowing the polar head to be oriented towards the aqueous continuous phase of the nanoparticle dispersion.

During the first two dialysis periods, conductivity in the receptor solution strongly increases which is indicative for a strong washing out-effect. During the third period, the conductivity increase is weaker and a plateau was reached after about 20 hours which was attributed to equilibrium of ions in the nanoparticle dispersion and the dialysate.

The total amount of CatA released from the nanoparticle dispersion, as determined from a calibration curve of conductivity as a function of CatA concentration, was 73.3 wt%. Thus, it can be inferred that the amount of CatA on the nanoparticle surface is about 26.7 wt%.

In **Table III** particle sizes and surface charges before and after dialysis are compared. TEM image analysis revealed that after dialysis, the mean nanoparticle size is slightly larger (about 30 nm) showing similar polydispersity. This size increase may be the result of a swelling of the polymer chains with time due to penetration of the aqueous continuous phase into the chains, enhanced by a wetting effect of the surfactants present in the nanoparticle dispersion. The nanoparticle shape remains globular which is presented in **Figure 6b**, a micrograph of the dialyzed nanoparticles. Size distributions of the nanoparticle dispersion before and after dialysis, as described in **Section 2.2.5**, are shown in **Figure 7**. Both size distributions have similar shapes. However, the size distribution after dialysis is shifted to larger particle sizes which could be explained by the earlier mentioned swelling effect.

Table III. Nanoparticle size (determined by TEM image analysis) and zeta potential (ξ) values of the nanoparticle dispersion obtained from a nano-emulsion of the Water / [CatA:Span® 80 =1:1] / [6 wt% EC10 in ethyl acetate] system with an O/S ratio of 70/30 and 90 wt% water, before and after dialysis.

	Mean diameter by TEM (nm)	**ζ (mV) diluted in water**	**ζ (mV) diluted in PB**

Before dialysis	228 ± 152	53.6	25.0
After dialysis	262 ± 180	24.3	-32.6

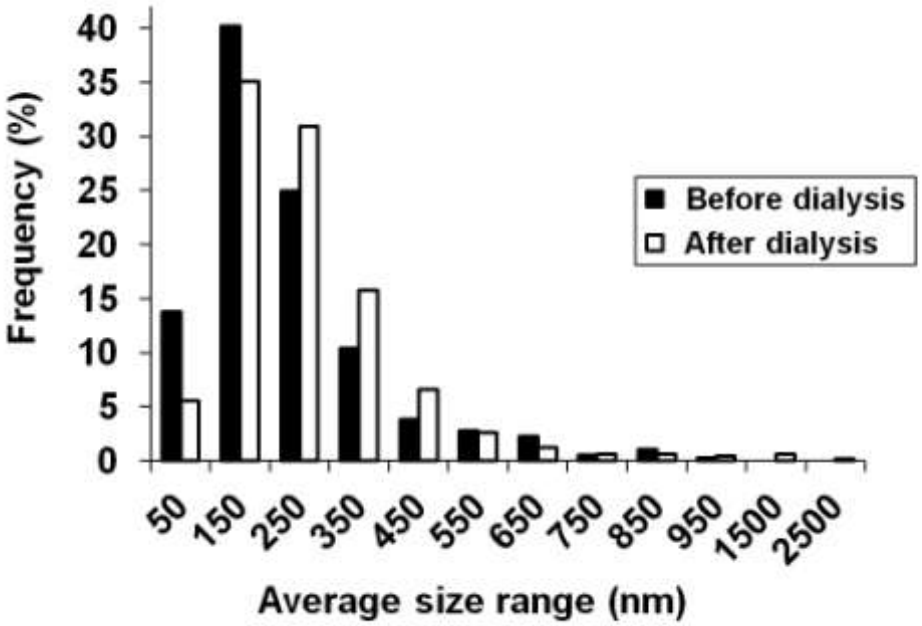

Figure 7: Nanoparticle size distribution assessed from TEM image analysis, of a nanoparticle dispersion obtained from a nano-emulsion of the Water / [CatA:Span® 80 =1:1] / [6 wt% EC10 in ethyl acetate] system with an O/S ratio of 70/30 and 90 wt% water, before and after dialysis.

With a value around +54 mV, the zeta potential value in water of the nanoparticles dispersion (**Table III**) was similar to that of the template nano-emulsion (**Table I**). This suggests that solvent evaporation has no influence on the surface charge of the system. These data confirm the hypothesis that the incorporation of the alkylamidoammonium derivative in the template ethylcellulose nano-emulsion is a suitable strategy to prepare nanoparticles with positive surface charge from nonionic polymers. Although zeta potential values are reduced to about half of the value after dialysis (+24 mV), they remain in the positive range. The reduction represents 45%, while the amount of CatA removed by dialysis was determined to be around 73 wt%,

as mentioned before. This supports the idea that positive surface charge may be attributed to the cationic surfactant strongly adsorbed on the nanoparticle surface. When diluting with PB buffer (as observed for the nano-emulsions), zeta potential values of the nanoparticle dispersion are significantly lower which is attributed to the interaction of the cationic charges at the nanoparticle surface with the anionic species of the PB buffer solution. After dialysis, zeta potential values are in the negative range (about -30 mV) which was associated with the shielding effect of the anions in the PB buffer as well as with the washing-off effect through dialysis.

4. CONCLUSIONS

Nano-emulsions containing ethylcellulose as oil component were formed in a mixed cationic:nonionic surfactant system by a low-energy emulsification method in a broad range of oil-to-surfactant (O/S) ratios. They showed a mean droplet diameter (ZAve) typically below 350 nm with a polydispersity below 0.15 and positive zeta potential values which were dependent on the pH of the diluting media. Droplet size of the nano-emulsions was reduced by the presence of oleylamine and higher zeta potential values were obtained. Stability assessment by light backscattering revealed that the main destabilization mechanism of the nano-emulsions in the absence of oleylamine may be creaming, while in the presence of oleylamine, other mechanisms such as Ostwald ripening may be mainly involved, which may explain their lower stability. However, the nano-emulsions were sufficiently stable for the preparation of nanoparticles by solvent evaporation. Nanoparticles obtained from the nano-emulsions with an O/S ratio of 70/30 without oleylamine showed a smaller mean diameter (about 250 nm) than the template nano-emulsion, and a high positive zeta potential (+54 mV). The microscopic appearance of the nanoparticle dispersion after dialysis suggests a globular core-shell-like morphology. When subjected to dialysis, the zeta potential values of the nanoparticles drop to the half of its original value, but keep the positive charge. This is attributed to the cationic surfactant strongly adsorbed on the nanoparticle surface or entrapped in its outer shell. These results confirm the hypothesis that positively charged nanoparticles can be obtained from ethylcellulose by a low-energy nano-emulsification-solvent evaporation approach using an alkylamidoammonium/Span 80 surfactant mixture in the emulsification step

and without the need of chemical reactions. This approach provides a simple way to endow positive charge to ethylcellulose nanoparticles.

ACKNOWLEDGEMENTS

Financial support from MINECO (grant CTQ2011-29336-C03-01) and Generalitat de Catalunya (grant 2009SGR-961) is acknowledged. CIBER-BBN is an initiative funded by the VI National R&D&i Plan 2008-2011, Iniciativa Ingenio 2010, Consolider Program, CIBER Actions and financed by the Instituto de Salud Carlos III with assistance from the European Regional Development Fund. S.L. is grateful to CIBER-BBN for a research scholarship. The DLS and Zeta potential analyses have been performed at the Nanostructured Liquid Characterization Unit, located at the Institute of Advanced Chemistry of Catalonia (IQAC), belonging to the Spanish National Research Council (CSIC) and affiliated to the NANBIOSIS ICTS of the CIBER-BBN. Prof. M.L. García of the Dept. of Physical-Chemistry at the Univ. of Barcelona is gratefully acknowledged for facilitating the use of TurbiscanLab® Expert. GPC analysis has been carried out at the Unitat de Tècniques Separatives i Síntesi de Pèptids of the CCiT-UB (University of Barcelona). Colorcon and Bonderalia S.A./Quimivita S.A. are gratefully acknowledged for the gift of ethylcellulose and ricinoleamidopropyltrimonium methosulfate respectively.

REFERENCES

[1] Hagigit T., Nassar T., Behar-Coehn F., Lambert G., Benita S., The influence of cationic lipid type on in-vitro release kinetic profiles of antisense oligonucleotide from cationic nanoemulsions. Eur J Pharm Biopharm 2008; 70: 248-259

[2] Tamilvanan S., Benita S., The potential of lipid emulsion for ocular delivery of lipophilic drugs. Eur. J. Pharm Biopharm 2004; 58 (2): 357-368.

[3] Fedeli E, Hernández-Aínsa S, Lancelot A, González-Pastor R, Calvo P, Sierra T and Serrano JL. Nanoobjects formed by ionic PAMAM dendrimers:

603 hydrophilic/lipophilic modulation and encapsulation properties. Soft Matter,
604 2015; 11: 6009 – 6017

605 [4] Saraswathi B, Balaji A and Umashankar MS. Polymers in mucoadhesive drug
606 delivery system-latest updates. International Journal of Pharmacy and
607 Pharmaceutical Sciences 2013: 5 (3): 423-430

608 [5] Timofeeva L, Kleshcheva N. Antimicrobial Polymers: Mechanism of Action,
609 Factors of Activity and Applications. Appl Microbiol Biotechnol 2011; 89: 475-
610 492

611 [6] Huh AJ, Kwon YJ. "Nanoantibiotics": A new paradigm for treating infectious
612 diseases using nanomaterials in the antibiotics resistant era. Journal of
613 Controlled Release 2011; 156: 128–145

614 [7] Sreekumar S, Goycoolea FM, Moerschbacher BM and Rivera-Rodriguez GR.
615 Parameters influencing the size of chitosan-TPP nano- and microparticles.
616 SCientifiC Reports 2018; 8:4695-4706 DOI:10.1038/s41598-018-23064-4

617 [8] Kesharwani P, Banerjee S, Gupta U, Amin MCIM, Padhye S, Sarkar FH, Iyer
618 AK. PAMAM dendrimers as promising nanocarriers for RNAi therapeutics.
619 Materials Today 2015; 18 (10): 565-572

620 [9] Fornaguera C, Grijalvo S, Galán M, Fuentes-Paniagua E, de la Mata FJ,
621 Gómez R, Eritja R, Calderó G, Solans C. Novel non-viral gene delivery
622 systems composed of carbosilane dendron functionalizae nanoparticles
623 prepared from nano-emulsions as non-viral carriers for antisense
624 oligonucleotides. Int J Pharm 2015; 478: 113-123

625 [10] Illum L., Jacobsen L.O., Müller R.H., Mak E., Davis S.S., Surface
626 characteristics and the interaction of colloidal particles with mouse peritoneal
627 macrophage. Biomaterials 1987; 8: 113 – 117.

628 [11] Gelperina S., Maksimenko O., Khalansky A., Vanchugova L., Shipulo E.,
629 Abbasova K., Berdiev R., Wohlfart S., Chepurnova N., Kreuter J., Drug
630 delivery to the brain using surfactant-coated poly(lactide-co-glycolide)
631 nanoparticles: Influence of the formulation parameters European Journal of
632 Pharmaceutics and Biopharmaceutics 2010; 74: 157–163.

633 [12] Tahara K., Yamamoto H., Kawashima Y., Cellular uptake mechanisms and
634 intracellular distributions of polysorbate 80-modified poly (D,L-lactide-co-

635 glycolide) nanospheres for gene delivery. Eur J Pharm Biopharm 2010; 75:
636 218–224.
637 [13] Gallardo V., Morales M.E., Ruiz M.A., Delgado A.V., An experimental
638 investigation of the stability of ethylcellulose latex Correlation between zeta
639 potential and sedimentation. Eur J Pharm Sci 2005; 26: 170–175.
640 [14] Freitas Ch., Müller H.R., Effect of light and temperature on zeta potential and
641 physical stability in solid lipid nanoparticle (SLN™) dispersions. International
642 Journal of Pharmaceutics 1998; 168: 221–229.
643 [15] Izquierdo P., Esquena J., TadrosT.F., Dederen C., Garcia M.J., Azemar N.,
644 Solans C., Formation and stability of nano-emulsions prepared using the
645 phase inversion temperature method. Langmuir 2002; 18: 26-30.
646 [16] Morales D., Gutiérrez J.M., García-Celma M.J., Solans C., A study of the
647 relation between bicontinuous microemulsions and oil/water nano-emulsion
648 formation. Langmuir 2003; 19, 7196-7200.
649 [17] Calderó C., García-Celma M.J., Solans C., Formation of polymeric nano-
650 emulsions by a low-energy method and their use for nanoparticle preparation.
651 J. Colloid Interf. Sci. 2011; 353: 406-411.
652 [18] Sadurní N., Solans C., Azemar N., García-Celma M.J., Studies on the
653 formation of W/O nano-emulsions, by low-energy emulsification methods
654 suitable for pharmaceutical applications. Eur J Pharm Sci 2005; 26 (5): 438-
655 445.
656 [19] Solè I., Maestro A., Pey C.M., González C., Solans C., Gutiérrez J.M., Nano-
657 emulsion preparation by low energy methods in an ionic surfactant system,
658 Colloid Surface A 2006; 288: 138-143.
659 [20] Maestro A., Solè I., González C. Solans C., Gutiérrez J.M., Influence of the
660 phase behavior on the properties of ionic nanoemulsions prepared by the
661 phase inversion composition method. J Colloid Interf Sci 2008; 327: 433-439.
662 [21] Solè I., Maestro A., González C., Solans C., Gutiérrez J. M., Optimization of
663 Nano-emulsion Preparation by Low-Energy Methods in a Ionic Surfactant
664 System. Langmuir 2006; 22: 8326-8332.
665 [22] Fritz G., Schädler V., Willenbacher N., Wagner N.J., Electrosteric Stabilization
666 of Colloidal Dispersions. Langmuir 2002, 18, 6381-6390
667 [23] Fornaguera C, Llinàs M, Solans C, Calderó G. Design and in vitro evaluation
668 of biocompatible dexamethasone-loaded nanoparticle dispersions, obtained

fromnano-emulsions, for inhalatory therapy. Colloids and Surfaces B: Biointerfaces 2015; 125: 58–64

[24] Calderó G., Montes R., Llinàs M., García-Celma M.J., Porras M., Solans C., studies on the formation of polymeric nano-emulsions obtained via low-energy emulsification and their use as templates for drug delivery nanoparticle dispersions. Colloids and Surfaces B: Biointerfaces 2016; 145: 922 – 931 DOI 10.1016/j.colsurfb.2016.06.013.

[25] Fornaguera C, Dols-Perez A, Calderó G, García-Celma MJ, Camarasa J, Solans C. PLGA nanoparticles prepared by nano-emulsion templating using low-energy methods as efficient nanocarriers for drug delivery across the blood–brain barrier. Journal of Controlled Release 2015; 211: 134–143

[26] Fornaguera C, Feiner-Gracia N, Calderó G, García-Celma MJ and Solans C. Galantamine-loaded PLGA nanoparticles, from nano-emulsion templating, as novel advanced drug delivery systems to treat neurodegenerative diseases. Nanoscale 2015; 7: 12076-12084

[27] Fornaguera C, Calderó G, Solans C. Electrolytes as a tuning parameter to control nanoemulsion and nanoparticle size. RSC Adv 2016; 6: 58203-58211

[28] Burgos-Mármol JJ, Solans C, Patti A. Effective short-range Coulomb correction to model the aggregation behaviour of ionic surfactants. J Chem Phys 2016; 144: 234904 DOI 10.1063/1.4954063

[29] Luxbacher Th. The Zeta Guide. Principles of the streaming potential technique. Anton Paar GmbH, Austria 2014. ISBN 978-3-200-03553-9

[30] Morral-Ruíz G., Solans C., García M.L., García-Celma M.J., Formation of Pegylated Polyurethane and Lysine-Coated Polyurea Nanoparticles Obtained from O/W Nano-emulsions. Langmuir 2012, 28, 6256−6264

[31] Meziani A., Zradba A., Touraud D., Clausse M., Kunz W., Can aldehydes participate in the nanostructuration of liquids containing charged micelles? J Mol. Liq. 1997; 73-74: 107-118.

[32] Clausse, M., Heil, J., Diffuse phase inversion, percolation and bicontinuous structures in microemulsions*, Lettere al Nuovo Cimento*, 1983, 36 (12), 369-376.

[33] Sahraneshin A., Takami S., Hojo D., Arita T., Minamid K., Adschiri T., Mechanistic study on the synthesis of one-dimensional yttrium aluminium garnet nanostructures under supercritical hydrothermal conditions in the presence of organic amines. Cryst Eng Comm, 2012, 14, 6085–6092

SUPPLEMENTARY INFORMATION

Suppl. Information 1: Determination of ethylcellulose molecular weight

The molecular weight of the ethylcellulose polymer was determined by Gel Permeation Chromatography. The experimental setup consisted on a Waters Alliance 2695 Separation Module equipped with a pump, an injector and a controller, and coupled to a Waters IR-2414 refractive index detector set at a sensibility of 128 A.U. and a temperature of 37 ºC. Two columns in series were used, namely a Styragel HR4 (300 x 7.8 mm) and a Styragel HR1 (300 x 7.8 mm). The eluent was tetrahydrofurane at a flux of 0.5 mL/min and the injection volume was 50 µL. Polystyrene standards for GPC were used for the calibration (Fluka; molecular weights of 3460; 27500; 62300 and 139000 Da). For the analysis, ethylcellulose was dissolved in tetrahydrofurane at a concentration of 5 mg/mL. The chromatogram was allowed to run for 55 minutes. Ethylcellulose retention time was 26 minutes. Sample was analyzed in duplicate.

Figure S1: Conductivity values as a function of time, measured in the dialysate (water) during dialysis of a nanoparticle dispersion obtained from a nano-emulsion of the Water / [CatA:Span® 80 =1:1] / [6 wt% EC10 in ethyl acetate] system with an O/S ratio of 70/30 and 90 wt% water, at a nanoparticle dispersion/dialysate ratio of 1/200, and changing dialysate after 30 and 150 minutes.

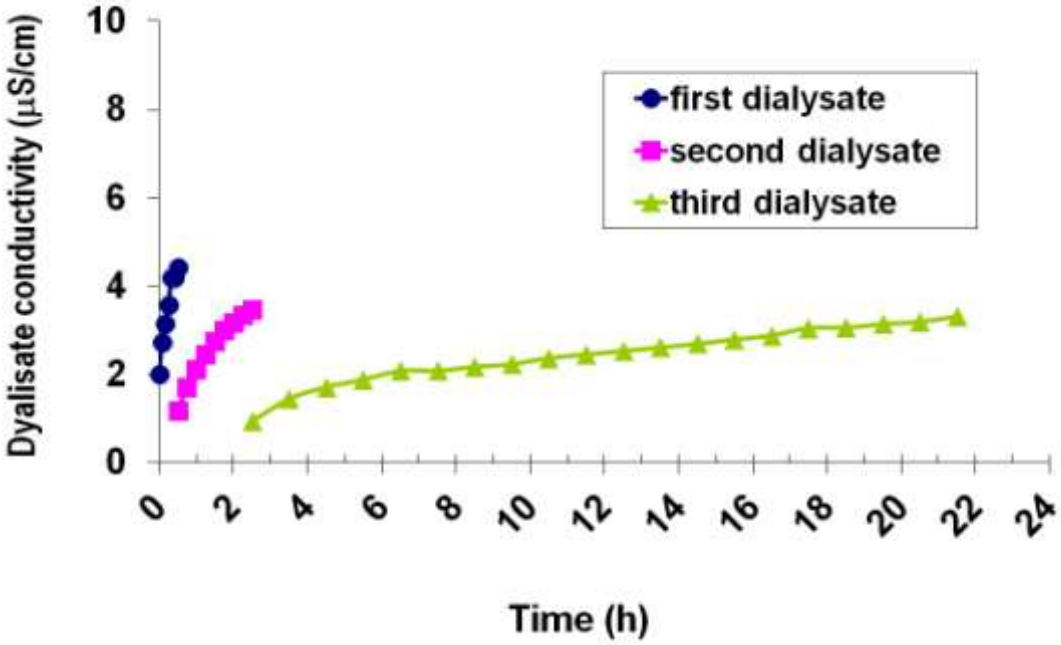
Dyalisate conductivity (µS/cm)
10
8
6
4
2
0
0
2
4
6
8
10
12
14
16
18
20
22
24
Time (h)
first dialysate
second dialysate
third dialysate

728